Confinement-Induced Orientational Order in a Ferroelectric Liquid Crystal Containing Dispersed Aerosils

George Cordoyiannis,[1] George Nounesis,[1] Vid Bobnar,[2] Samo Kralj,[2,3] and Zdravko Kutnjak[2]
[1]National Centre for Scientific Research "Demokritos", 153 10 Aghia Paraskevi, Greece
[2]Jožef Stefan Institute, P.O. Box 3000, 1001 Ljubljana, Slovenia
[3]Faculty of Education, University of Maribor, 2000 Maribor, Slovenia
(Received 12 June 2004; published 18 January 2005)

The study of the smectic-A to chiral smectic-C^* phase transition of the liquid crystal S-(+)-[4-(2′-methyl butyl) phenyl 4′-n-octylbiphenyl-4-carboxylate] (CE8) containing dispersed hydrophilic aerosils reveals novel properties, important to understanding quenched disorder and confinement in ferroelectric liquid crystals. Smectic layer compression leads to a distribution of transition temperatures inducing smearing of the macroscopic data across the transition. A pronounced confinement-induced pretransitional tilted order is observed.

DOI: 10.1103/PhysRevLett.94.027801 PACS numbers: 61.30.–v, 65.20.+w, 61.10.–i

A wide range of physical systems, from superfluid ^{4}He in aerogels and porous glasses to doped semiconductors, have attracted considerable experimental and theoretical efforts aiming at understanding the effects of quenched random disorder (QRD) upon phase transitional behavior. Liquid crystals (LCs) are ideal for QRD studies [1]. They are soft systems exhibiting strong responses to relatively weak perturbations. Moreover, they exhibit a rich variety of mesophases involving long-range transitional and/or orientational molecular ordering. Over the past ten years, studies have been primarily focused upon the Isotropic (I)-Nematic (N) [2] as well as the N-Smectic-A (SmA) transition [2,3]. The effects of quenched disorder on coarsening dynamics of liquid crystals have also been studied [4]. Various ''disordering agents'' have been employed either as confining matrices (controlled pore glasses, Vycor glasses, aerogels) [5] or inclusions (aerosil nanoparticles) [6]. So far, a good agreement between the theoretical random-field approach (based upon pinning the phase of the smectic density wave) [7] and experimental findings has been demonstrated in the case of tricritical-like N-SmA transitions [3]. Finite correlation lengths have been measured in the SmA phase in the presence of even the smallest amount of disorder [8]. Also, with increasing strength of the quenched disorder [3], a crossover to critical 3D-XY-like behavior has been observed near the pseudo N-SmA transition temperature T_C.

Recently, the attention was shifted to the continuous mean-field-like SmA-Smectic-C (SmC) phase transition. While theoretical predictions have not yet been formulated, the experimental evidence points towards a minimization of the random disorder effects, possibly due to the long-range interactions driving the transition. The recently published x-ray diffraction experiments [9] on mixtures of $\overline{8}S5$ with silica nanoparticles revealed that the weak coupling of the liquid crystal with the hydrophilic aerosil surface does not influence the overall molecular orientation and the character of the transition [9]. Contrary to these results, dielectric spectroscopy measurements on the SmA-SmC^* phase transition of the liquid crystal S-(+)-[4-(2′-methyl butyl) phenyl 4′-n-octylbiphenyl-4-carboxylate] (CE8) containing dispersed silica aerosils demonstrated that aerosils strongly affect the transitional behavior [10]. The soft mode characteristic frequency was found to be consistent with a crossover behavior from mean-field tricritical to 3D-XY, as the value of aerosil concentration increased. However, the uncertainty associated with the experimental critical exponents derived from data extensively smeared near T_C was quite large to undoubtedly prove the QRD predictions. Moreover, additional intriguing features were observed [10]: (i) The temperature dependence of the characteristic Goldstone mode frequency remains bulklike while the corresponding soft mode data are smeared with increasing aerosil concentration. (ii) At T_C, an unexpected discontinuity is induced between the soft and Goldstone mode relaxation frequencies. (iii) In the stiff confinement regime, the Goldstone mode becomes totally suppressed indicating the disappearance of the helicoidal structure of the tilted phase, while the liquid crystal could not be aligned in the presence of an external magnetic field [11].

In order to explore the effects of the strong liquid crystal-aerosil coupling upon the SmA-SmC^* phase transition, we have carried out powder x-ray diffraction measurements of the tilt angle $\theta(T)$ and ac calorimetric measurements of $C_p(T)$ across the transition of aerosil-CE8 mixtures as a function of aerosil concentration x ($x = m_s/(m_s + m_{lc})$, m_s and m_{lc} stand for the mass of the aerosil and the liquid crystal, respectively). The hydrophilic coating of the aerosil surface produces strong homeotropic anchoring of the polar CE8 molecules [12]. Our results reveal new phenomena important for understanding aerosil-induced QRD in liquid crystals: (i) Smectic layer compression leading to a distribution of

layer thickness and thus of transition temperatures is responsible for the broadening of macroscopic data across the transition. (ii) Pretransitional tilted order appears, becoming increasingly pronounced with the degree of confinement. Analogous surface-induced pretransitional behavior has recently been reported by Syed and Rosenblatt [13], involving two competing easy axes for liquid crystal alignment.

The liquid crystal CE8 was supplied by Merck and was used without any additional treatment. The hydrophilic aerosils 300 (spherical SiO_2 particles, $2R \sim 7$ nm), treated with hydroxyl groups were manufactured by Degussa. The CE8-aerosil mixing procedure has been described elsewhere [6,8]. After mixing and until loading for the experiments the samples were kept at 95 °C in order to avoid aerosil-LC demixing due to recrystallization [6]. For the x-ray diffraction measurements the Cu K_α line was used from a Rigaku RUH3R rotating anode source operating at 5 kW. Flat graphite was used as monochromator while point focusing of the beam (0.5 mm) was attained by double focusing mirrors (Molecular Structure Corporation) housed in a continuous He flow environment. The 2D detector is the Molecular Structure Corporation R-Axis IV (30×30 cm^2) double imaging plate system. The resolution was 4.0×10^{-3} Å^{-1} half width at half maximum. The samples were loaded in glass capillary tubes at 95 °C and mounted on a heating stage with temperature stability ± 0.01 K (Instec Inc.). The samples were instantly heated to the isotropic phase (417.5 K) and then cooled to SmA for measurements at selected temperatures.

Powder scattering profiles of the normalized x-ray intensity versus wave vector transfer were collected for samples with $x = 0$, 0.05, 0.10, and 0.15 at various temperatures in the SmA and SmC^* phases. The instrumental resolution does not allow for the detailed line shape analysis carried out by Clegg *et al.* for the SmA-SmC transition of $\overline{8}S5$ [9]. Figure 1 illustrates the line shapes in the SmA [$\sim$1.5 K above T_C, Fig. 1(a)] and in the SmC^* phase [$\sim$7 K below T_C, Fig. 1(b)]. The broadening of the x-ray peaks relative to the bulk can readily be observed. As shown in the insets of Fig. 1, the width of the quasi-Bragg peaks increases abruptly for $x = 0.05$ and remains relatively constant for $x = 0.10$ and 0.15. The values of the smectic correlation lengths (ξ) obtained at $(T - T_C) = 1.5$ K are 420 ± 20 Å for $x = 0.05$, 340 ± 30 Å for $x = 0.10$, and 330 ± 30 Å for $x = 0.15$. The corresponding values for the average open length l_0, where $l_0 = 2/a\rho_s$ [ρ_s is the mass of silica per cm^3 of LC and a is the active surface area of the aerosils ($a = 300 \pm 30$ m^2 g^{-1})] [3]: $l_0 = 1260$ Å for $x = 0.05$, $l_0 = 600$ Å for $x = 0.10$, and $l_0 = 380$ Å for $x = 0.15$. It is evident that $\xi < l_0$ for any value of x. Thus, the origins of the broadening of the smectic diffraction peaks cannot be attributed solely to the dimensions of the confining cavity. Analogously to the SmA-SmC transition [9], the temperature dependence of the correlation lengths $\xi(T)$ shows a slightly decreasing

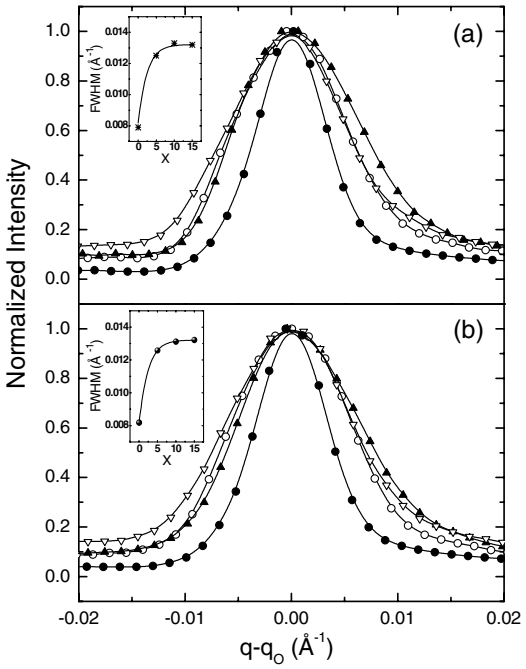

FIG. 1. Line shapes for the bulk CE8 (solid circles) and three aerosil mixtures $x = 0.05$ (open circles), 0.10 (solid triangles), and 0.15 (open triangles) taken in SmA phase, $T - T_C = 1.5$ K (a) and SmC^* phase, $T_C - T = 7$ K (b). The insets in (a) and (b) show the FWHM of the quasi-Bragg peaks as a function of the aerosil concentration x.

trend in the SmA upon cooling towards T_C, while remaining finite and relatively constant in the SmC^* phase.

The $\theta(T)$ profiles can be straightforwardly extracted from $\theta(T) = \arccos[d(T)/d_A(T)]$, where $d(T)$ is the temperature dependent smectic layer thickness and $d_A(T)$ the corresponding thickness in the SmA phase well above T_C. The results for the bulk sample as well as for $x = 0.05$ and 0.10 are presented in Fig. 2. The data for bulk CE8 are in good agreement with previously published results [14]. The data for $x = 0.05$ and 0.10 clearly deviate from the bulk behavior. They exhibit a substantial decrease of the magnitude of θ deep in the SmC^* phase as well as smearing of the $\theta(T)$ data near T_C, within a T range increasing with x. Considering T_C values measured by dielectric spectroscopy [10] and calorimetry, it can be claimed that nonzero molecular tilt exists for both aerosil mixtures at $T > T_C^{\text{bulk}}$ (where T_C^{bulk} stands for T_c of bulk CE8). $\theta(T)$ profiles are fit by an extended mean-field model [15]. Successful fits for $x = 0.05$ and 0.10 could be achieved after the omission of smeared data near T_C (Fig. 2). The $\theta(T)$ profiles demonstrate trends with x, in contrast with the findings by Clegg *et al.* for the SmA-SmC phase transition of $\overline{8}S5$ where the corresponding $\theta(T)$ profiles could be scaled in their entirety, for all the values of aerosil concentration studied [9]. As illustrated in Fig. 3, deviations from bulk behavior are dramatically enhanced for $x = 0.15$. Even at temperatures high above the SmA-SmC^* transition the smectic layers are substantially compressed

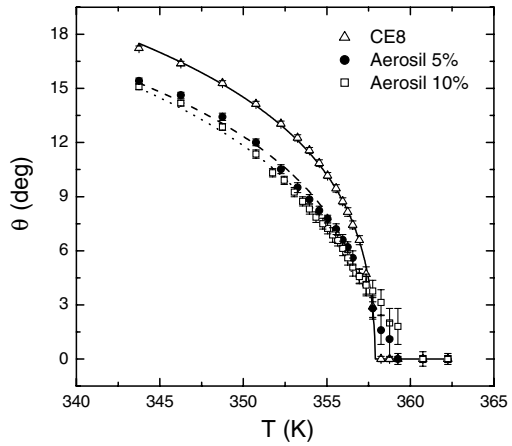

FIG. 2. Tilt angle $\theta(T)$ for the bulk CE8 (open triangles) and two aerosil mixtures $x = 0.05$ (solid circles) and $x = 0.10$ (open boxes) across the SmA-SmC^* transition. Solid, dashed, and dotted lines represent the results of fits to the extended mean-field model [15].

[Fig. 3(a)]. $d_A = d(T > 366\ \mathrm{K})$ has been used to calculate $\theta(T)$ [data presented in Fig. 3(b)]. The temperature profile of the tilt is characterized by a high degree of broadening for a wide T range and a pronounced wing extending for several degrees above T_C^{bulk}.

Details of the ac calorimetric technique have been published elsewhere [16]. The obtained C_p anomalies are illustrated in Fig. 4. They demonstrate the strong impact of aerosil concentration upon the transition. The data for bulk CE8 exhibit the characteristic mean-field tricritical behavior observed in the vicinity of SmA-SmC^* phase transitions [15]. The $x = 0.05$ C_p peak is broadened while demonstrating an excess C_p wing extending at high temperatures. The measured T_C shift is comparable to the results from dielectric spectroscopy. Finally, the C_p anomalies for $x = 0.10$ and $x = 0.15$ are severely broadened and could not be analyzed further.

The $\theta(T)$ and $C_p(T)$ data for the SmA -SmC^* transition presented in this Letter demonstrate the strong influence of confinement upon the character of the transition. The behavior observed for SmA-SmC was attributed to long-range interactions driving the transition that were likely to minimize the impact of QRD upon the orientational order [9]. Different scenarios have to be adopted in order to understand the present data. One such scenario was proposed to describe the dielectric spectroscopy results in-

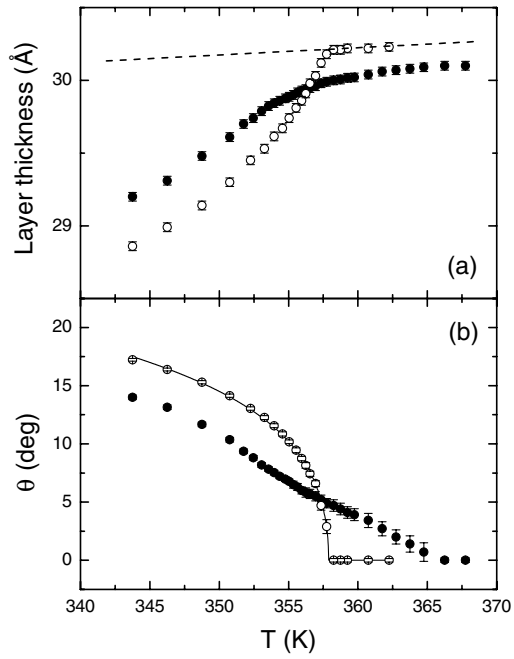

FIG. 3. (a) Smectic layer thickness d as a function of temperature for the bulk CE8 (open circles) and the aerosil mixture $x = 0.15$ (solid circles). The dashed line denotes extrapolated temperature dependence of the bulk SmA layer thickness background. (b) Tilt angle $\theta(T)$ for the bulk CE8 (open circles) and the aerosil mixture $x = 0.15$ (solid circles). Solid line denotes the fit to the extended mean-field model [15].

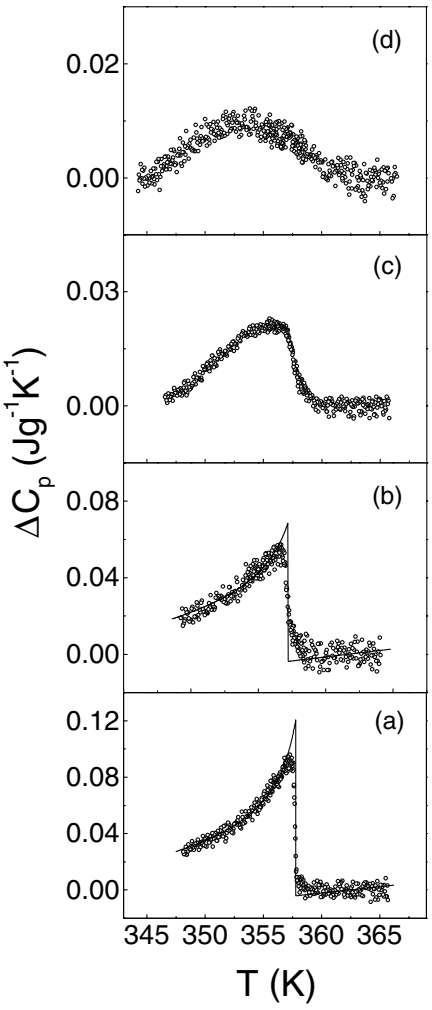

FIG. 4. Excess heat capacity as a function of temperature for bulk CE8 (a) and three aerosil mixtures $x = 0.05$ (b), 0.10 (c), and 0.15 (d). Solid lines in (a) and (b) represent the result of a fit to the extended mean-field model [15].

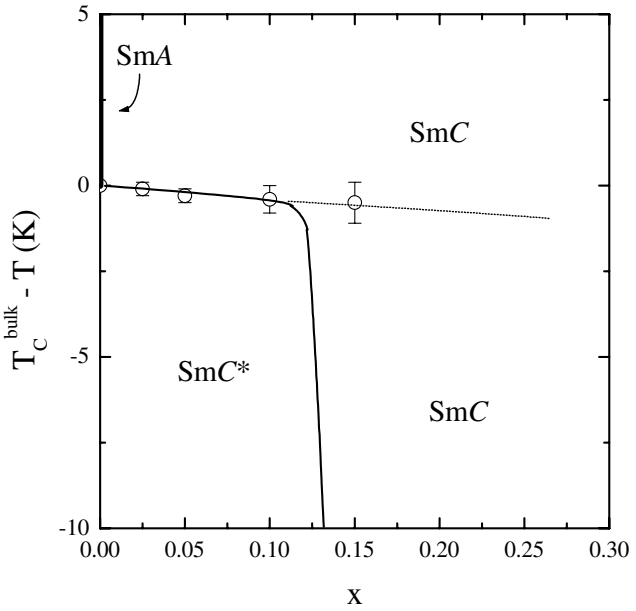

FIG. 5. Schematic $T - x$ phase diagram based on dielectric, heat capacity, and x-ray experiments. The dotted line represents the supercritical-like locus at which the fastest changes in physical parameters take place during continuous evolution within the homogeneous SmC phase.

volving the smearing of the soft mode susceptibility data caused at high x, as well as the discontinuous gap found between the soft and the Goldstone mode relaxation frequencies at T_C [10]. These findings were associated to a possible T_C distribution originating from the strong LC-aerosil interaction inducing a corresponding distribution of the smectic layer thickness [10]. The x-ray diffraction results obtained here provide evidence for the validity of this proposal.

A substantial suppression of the layer thickness in the stiff confinement regime ($x = 0.15$) leads to the most notable characteristic of the $\theta(T)$ profiles, the existence of tilted order for several degrees above T_C^{bulk} ($\sim$8 K), which is analogous to the case of electric field-induced pretransitional tilt. Pinning of the critical fluctuations by the rigid aerosil network is effectively cooling the system towards the critical point at which the confinement-induced ordering field can easily establish tilted order at temperatures well above the T_C^{bulk}.

Parallels can be drawn between the aerosil mixtures studied here and the observed behavior of ferroelectric LCs in the presence of the conjugate ordering field to the tilted order (i.e., the external electric field, E). In both cases, pretransitional orientational order would be induced. Furthermore, the $T - x$ phase diagram can be constructed as an analogue to the $E - T$ phase diagram [17]. Such a phase diagram is presented in Fig. 5. As demonstrated by the existence of the Goldstone mode [10], the SmC^* phase can only exist at low T and x in the soft regime ($x \leq 0.10$). At higher temperatures, in the light of the present data, a homogeneous SmC phase (without helicoidal structure) should exist for all $x \neq 0$. The SmA phase, bearing no trace of tilted order, would only exist at $x = 0$. As it can be deduced from Fig. 5, in the stiff confinement regime ($x > 0.10$) the same symmetry manifests at all T and so the data presented here at $x = 0.15$ do not correspond to a real phase transition but rather to a mere evolution of the magnitude of the pinned tilted order characterized by an almost completely suppressed and broadened C_p anomaly.

Research supported by the Greek-Slovene Bilateral Scientific and Technological Cooperation Project No. GR 20/2003, the General Secretariat for Research and Technology of Greece, and the Slovenian Office of Science under Program No. P1-0125 and Project No. J1-6593-0106-04. Technical assistance from the Center for Crystallography of Macromolecules at N.C.S.R. ''Demokritos'' is acknowledged.

[1] T. Bellini, L. Radzihovsky, J. Toner, and N. A. Clark, Science **294**, 1074 (2001).
[2] T. Bellini, N. A. Clark, C. D. Muzny, L. Wu, C. W. Garland, D. W. Schaefer, and B. J. Olivier, Phys. Rev. Lett. **69**, 788 (1992).
[3] G. S. Iannacchione, C. W. Garland, J. T. Mang, and T. P. Rieker, Phys. Rev. E **58**, 5966 (1998).
[4] D. K. Shenoy, J. V. Selinger, K. A. Grüneberg, J. Naciri, and R. Shashidhar, Phys. Rev. Lett. **82**, 1716 (1999).
[5] D. Cleaver, S. Kralj, T. Sluckin, and M. Allen, *Liquid Crystals in Complex Geometries Formed by Polymer and Porous Networks* (Taylor and Francis, London, 1996).
[6] H. Haga and C. W. Garland, Phys. Rev. E **56**, 3044 (1997).
[7] L. Radzihovsky and J. Toner, Phys. Rev. B **60**, 206 (1999).
[8] R. L Leheny, S. Park, R. J. Birgeneau, J.-L. Gallani, C. W. Garland, and G. S. Iannacchione, Phys. Rev. E **67**, 011708 (2003).
[9] P. S. Clegg, R. J. Birgeneau, S. Park, C. W. Garland, G. S. Iannacchione, R. L. Leheny, and M. E. Neubert, Phys. Rev. E **68**, 031706 (2003).
[10] Z. Kutnjak, S. Kralj, and S. Žumer, Phys. Rev. E **66**, 041702 (2002).
[11] Z. Kutnjak, G. Cordoyiannis, and G. Nounesis, Ferroelectrics **294**, 105 (2003).
[12] M. Marinelli, A. K. Ghosh, and F. Mercuri, Phys. Rev. E **63**, 061713 (2001).
[13] I. M. Syed and C. Rosenblatt, Phys. Rev. E **68**, 031701 (2003).
[14] Z. Raszewski, J. Rutkowska, J. Kedzierski, P. Perkowski, W. Piecek, J. Zielinski, J. Zmija, and R. Dabrowski, Mol. Cryst. Liq. Cryst. Sci. Technol., Sect. A **263**, 271 (1995).
[15] S. Dumrongrattana, G. Nounesis, and C. C. Huang, Phys. Rev. A **33**, 2181 (1986).
[16] H. Yao, K. Ema, and C. W. Garland, Rev. Sci. Instrum. **69**, 172 (1998); Z. Kutnjak, S. Kralj, G. Lahajnar, and S. Žumer, Phys. Rev. E **68**, 021705 (2003).
[17] K. Kondo, Y. Sato, H. Takezoe, A. Fukuda, and E. Kuze, Jpn. J. Appl. Phys. **20**, L871 (1981).